cancers

MDPI

Communication

Trametinib and Fimepinostat Induce Malignant Peripheral Nerve Sheath Tumor Cell Death *In Vitro*

Ethan W. Hass, Sofia A. Oliveira and Cristina Fernandez-Valle *

Burnett School of Biomedical Sciences, College of Medicine, University of Central Florida, Orlando, FL 32816, USA
* Correspondence: cfv@ucf.edu; Tel.: +1-(407)-266-7033

Simple Summary

Malignant peripheral nerve sheath tumors are deadly tumors that develop in patients with Neurofibromatosis Type 1 (NF1). There are currently no effective treatments for these tumors, and NF1 patients with MPNSTs face bleak odds of survival including death in adolescence and early adulthood. New drugs currently entering clinical trials for MPNSTs include inhibitors of MEK and HDAC enzymes. The authors present evidence that the MEK inhibitor trametinib and dual HDAC/PI3K inhibitor fimepinostat could be more efficacious in MPNST patients than the drugs currently under clinical investigation. This conclusion is supported by timelapse imaging data collected from nine unique patient-derived MPNST cell lines. The results presented here confirm previous preclinical studies and a case report and inform future MPNST clinical trials.

Abstract

Background/Objectives: Neurofibromatosis Type 1 (NF1) is a genetic syndrome caused by pathogenic *NF1* variants encoding neurofibromin, a Ras GTPase activating protein. Individuals with NF1 develop peripheral nerve sheath tumors called neurofibromas. Approximately 50% of NF1 patients develop plexiform neurofibromas (pNFs) which have up to 13% lifetime risk of transformation into malignant peripheral nerve sheath tumors (MPNSTs). Current therapeutic strategies emphasize surgical resection with wide margins, radiation, and traditional chemotherapy for unresectable MPNSTs. However, NF1 patients diagnosed with MPNSTs have 5-year survival rates as low as 16%. The two recently FDA-approved drugs for pNFs, the MEK inhibitors selumetinib and mirdametinib, are not used to prevent or treat MPNSTs. Methods: The MEK inhibitor trametinib and the dual HDAC/PI3K inhibitor fimepinostat were assessed for growth inhibitory effects in nine unique patient-derived MPNST cell lines, as both drugs have preclinical efficacy in other Schwann cell-derived tumors. Results: Trametinib, which is approved for malignant melanomas, promoted cell death in 7/9 MPNST cell lines with a geometric mean GI50 = 17 nM. When directly compared to selumetinib and mirdametinib in a subset of four MPNST cell lines, trametinib had the lowest mean GI50 (trametinib = 38 nM, mirdametinib = 1.6 μM, selumetinib = 4.9 μM). Trametinib was also superior to selumetinib and mirdametinib in blocking ERK1/2 phosphorylation for 24 h. Fimepinostat promoted cell death in all cell lines with a geometric mean GI50 = 17 pM. Conclusions: These studies demonstrate *in vitro* efficacy for two candidate MPNST therapeutics which could reduce tumor burden and metastasis in NF1 patients.

Keywords: neurofibromatosis; NF1; malignant peripheral nerve sheath tumor; trametinib; mirdametinib; selumetinib; fimepinostat; MEK; HDAC; drug sensitivity assays

Check for updates

Academic Editors: Mohamed S. Abdelbaki and Nicole Brossier

Received: 5 December 2025
Revised: 18 February 2026
Accepted: 20 February 2026
Published: 26 February 2026

Copyright: © 2026 by the authors. Licensee MDPI, Basel, Switzerland. This article is an open access article distributed under the terms and conditions of the Creative Commons Attribution (CC BY) license.

1. Introduction

Neurofibromatosis Type 1 (NF1) is a genetic syndrome caused by loss of function in *NF1* encoding the Ras GTPase-activating protein neurofibromin [1]. NF1 affects approximately 1 in 3000 individuals [2]. Those affected display a wide range of manifestations with highly variable expressivity including peripheral nerve tumors, optic gliomas, iris hamartomas (Lisch nodules), skin pigmentary abnormalities, musculoskeletal malformations, cognitive deficits, and gastrointestinal, hematopoietic, and endocrine malignancies [3,4]. Chief among the neoplastic manifestations are neurofibromas, benign nerve tumors that contain an admixture of neoplastic Schwann cells, fibroblasts, perineurial-like cells, and residual axons [5]. Up to 50% of NF1 patients develop large, plexiform neurofibromas (pNFs) that involve multiple nerve fascicles, cause disfigurement and disability and have a 6–13% lifetime risk of transformation into malignant peripheral nerve sheath tumors (MPNSTs) [5–8]. Individuals with severe phenotypes arising from *NF1* microdeletions or missense mutations in codons 844–848 have a higher lifetime risk of MPNST development [9,10]. These patients are also likely to develop more neurofibromas at a younger age [10], and many die from MPNSTs in adolescence [11–13].

MPNSTs are diverse in their origin and genetic characteristics. Approximately half of all MPNSTs develop from NF1-related pNFs, with the other half occurring spontaneously or from previous radiotherapy [14]. Loss of *CDKN2A/B* is often an early event causing pNFs to become premalignant atypical neurofibromatous neoplasms of uncertain biological potential (ANNUBP) [15,16]. Additional somatic mutations or copy number changes in PRC2 components *SUZ12* and *EED* [17,18], *TP53* [19], *PTEN* [20], and many other genes [21] promote ANNUBP transformation into MPNSTs. Due to the diverse genetic composition of MPNSTs, there are presently no universal biomarkers that predict efficacy for candidate targeted therapeutics [22]. However, recent multi-omic analyses revealed that distinct subgroups of MPNSTs exist, each with different predicted vulnerabilities in either the SHH or WNT/β-catenin/CCND1 pathways [23]. Histopathologic studies have also identified MPNST subgroups with distinct responses to radiation therapy based on histone H3 trimethylation, neurofibromin, S100, SOX10, p16, and EGFR immunoreactivity [24].

NF1-related MPNSTs have worse prognoses than non-NF1-related MPNTS, with 16–38% overall 5-year survival rates versus approximately 60%, respectively [25–27]. Current therapeutic strategies for MPNSTs emphasize complete surgical resection with negative margins [27], but recurrence rates remain as high as 70% [28]. Radiotherapy is also used for local MPNST control but has not been found to improve survival [29]. The current standard of care for unresectable or remittent MPNSTs is traditional chemotherapeutics (SARC006 protocol). Clinical trials (summarized in Table 1) have evaluated small molecule inhibitors for MPNSTs, although no drugs have been FDA-approved for this indication. Notably, two MEK inhibitors approved for unresectable NF1-related pNFs, selumetinib (Koselugo) and mirdametinib (GoMEKLI), are entering clinical trials as part of combination therapies for MPNSTs (NCT06735820, NCT05253131, NCT06693284). Recent preclinical studies identified another FDA-approved MEK inhibitor, trametinib (Mekinist) as more effective *in vitro* than selumetinib and mirdametinib [30]. We reported similar observations in human and mouse schwannoma model cells [31,32]. A recent precision medicine case study demonstrated trametinib's clinical efficacy in treating a recurrent pediatric MPNST [33]. High-throughput screening campaigns have also identified HDAC inhibitors as potent compounds in patient MPNST cell lines [34,35]. Our previous work demonstrated the dual HDAC/PI3K inhibitor fimepinostat promotes apoptosis in *NF2*-related schwannoma cells [36,37]. With these data in mind and nine distinct MPNST cell lines available for study, we compared the *in vitro* efficacies of trametinib, mirdametinib, selumetinib, and fimepinostat using high-content live cell imaging over 5 days.

Table 1. Past, current, and planned MPNST clinical trials.

Completion Date (Actual or Estimated)	NCT Number	Phase	Interventions	Mechanism	Results
08/2009	NCT00068367	2	erlotinib hydrochloride	EGFR inhibitor	Completed, no responders (0/20), all pretreated with other chemotherapies
06/2014	NCT00304083	2	doxorubicin hydrochloride, etoposide, ifosfamide	DNA intercalator, topoisomerase inhibitor, alkylating agent	Completed, partial response in 5/28 NF1 cases
12/2017	NCT01661283	1/2	everolimus, bevacizumab	mTOR inhibitor, anti-VEGF monoclonal antibody	Completed, clinical benefit rate = 12%
07/2018	NCT02008877	2/3	ganetespib, sirolimus	HSP90 inhibitor, mTOR inhibitor	Completed, progressive disease in all NF1 cases (8)
04/2009	NCT00427583	2	imatinib mesylate	BCR-ABL inhibitor	Terminated, slow recruitment and no effect
5/17/2018	NCT02986919	1	CPI-0610 (pelabresib)	Bromodomain and extra-terminal domain inhibitor	Terminated, lack of enrollment
12/2020	NCT02691026	2	pembrolizumab	anti-PD-1 monoclonal antibody	Terminated, slow enrollment due to low incidence of MPNST and the COVID-19 pandemic.
10/1/2023	NCT03433183	1	selumetinib, sirolimus	MEK inhibitor, mTOR inhibitor	Completed, results not published
2/2/2024	NCT05011019	1/2	AL2846	c-MET inhibitor	Terminated, sponsor adjusts its research and development strategy
10/1/2024	NCT02584647	2	PLX3397, sirolimus	CSF1R inhibitor, mTOR inhibitor	Terminated, poor enrollment
7/30/2025	NCT04465643	EARLY 1	nivolumab ipilimumab	anti-PD-1 monoclonal antibody, CTLA-4 monoclonal antibody	Completed, no results posted
-	NCT05107037	2	TQ-B3234	MEK inhibitor	unknown
1/1/2026	NCT06693284	2	mirdametinib and vorinostat	MEK inhibitor, HDAC inhibitor	recruiting
01/2026	NCT04917042	1/2	tazemetostat	EZH2 inhibitor	active, not recruiting
4/16/2026	NCT03872427	2	telaglenastat hydrochloride	glutaminase inhibitor	active, not recruiting
04/2026	NCT04872543	2	decitabine, cedazuridine	cytidine analog, cytidine deaminase inhibitor	recruiting
10/1/2028	NCT06735820	2	APG-115, selumetinib	MDM2 inhibitor, MEK inhibitor	not yet recruiting
05/15/2032	NCT05253131	2	selumetinib, unnamed bromodomain inhibitor, durvalumab	MEK inhibitor, bromodomain inhibitor, anti-PD-L1 monoclonal antibody	not yet recruiting

2. Materials and Methods

2.1. MPNST Cell Culture

Human patient-derived MPNST cells (Table 2) were received from Drs. Steven Caroll and Jody Longo at the Medical University of South Carolina, Dr, George DeVries at the McGuire VA Medical Center and Dr. Margaret Wallace at the University of Florida and frozen in liquid nitrogen until use in this study. MPNST cells were originally isolated from patient tissues by mechanical and/or enzymatic digestion and grown *in vitro* for multiple passages without any reported further modification or immortalization [38–45]. Once thawed, MPNST cells were all grown on T75 flasks with CellBind growth surfaces (Corning, NY, USA) in Dulbecco's modified eagle medium (DMEM; Thermo Fisher, Waltham, MA, USA) with 10% heat-inactivated fetal bovine serum (FBS; R&D Systems, Minneapolis, MN, USA) and 100 U/mL penicillin–streptomycin (Thermo Fisher, Waltham, MA, USA) and incubated at 37 °C, 5% CO_2 until confluent.

Table 2. MPNST cell lines studied.

MPNST Cell Line	Patient Age/Sex	Tumor Origin	NF1 vs. Sp [1]	Tumor *NF1* Status	Primary vs. Metastatic	Stage	References
sNF96.2	27 M	Lower Extremity	NF1	NF1 -/-	Primary	High-grade MPNST	[38,39]
S462	19 F	Thigh	NF1	NF1 -/-	Primary	High-grade MPNST	[40]
NMS-2 [2]	30 M	Thigh	NF1	NF1 -/-	Primary	High-grade MPNST	[41]
ST88-14	24 M	Retroperitoneal	NF1	NF1 -/-	Primary	High-grade MPNST	[42]
2XSB	57 F	Brachial nerve	Sp	NF1 + (protein)	Primary	High-grade sporadic MPNST	[43]
sNF02.2	35 M	Lung	NF1	NF1 + (protein)	Metastatic	Benign and premalignant (plexiform)	[38]
NMS-2PC [2]	30 M	Retroperitoneal	NF1	NF1 -/-	Metastatic	Metastatic MPNST	[41]
sNF94.3	43 M	Lung	NF1	NF1 -/- (microdeletion)	Metastatic	Benign and premalignant (plexiform)	[38]
NFS-1	N/A	Not Specified	NF1	NF1 -/-	N/A	High-grade MPNST	[40]
STS-26T [3]	51 F	Scapula	Sp	NF1 + (protein)	Metastatic	BRAF V600E Melanoma	[44,45]

[1] Sp = sporadic, non-NF1-related. [2] Cell lines were isolated from two distinct tumors resected from the same patient. [3] Reclassified as BRAF V600E-mutant melanoma, originally classified as a sporadic MPNST.

2.2. High-Content Drug Sensitivity Assay

After at least two passages post-thawing, each MPNST cell line was trypsinized and 1000 cells were seeded per well in CellBind 384-well plates (Corning, NY, USA) in 20 µL DMEM + 10% FBS. Cells were allowed to attach overnight at 37 °C, 5% CO_2 and were treated the following day. Treatment was facilitated using the Integra Assist automated pipetting robot (Princeton, NJ, USA) programed to perform ten-fold serial dilutions for each drug (10 µM to 10 fM) in DMEM + 10% FBS. Prepared drug solutions were added to each well of the 384-well plate in 10 µL at 3× concentration (final volume per well = 30 µL). All compounds tested in the high-content assay were obtained from Selleck Chemicals (Houston, TX, USA) and stored as stock solutions at −80 °C in DMSO at 10 mM. Immediately after treatment, the 384-well plates were placed in the Incucyte live cell imaging system (Sartorius, Göttingen, Germany) and incubated at 37 °C, 5% CO_2 with images captured in each well every 4 h for 120 h.

The high-content assay uses cellular confluence in each well as a composite metric for average cell size and cell proliferation over time. Percent cellular confluence in each well of the 384-well plate was estimated every 4 h using the Incucyte software version 2025B (Sartorius). Change in percent confluence from the time drug treatment was initiated was plotted for all drug doses in each cell line. To quantitate drug efficacy in reducing cellular confluence, the area under the confluence curve (AUC) was plotted for each dose. Using the AUC dose–response curves, relative 50% growth inhibitory concentrations (GI50s) were determined for all drugs in each cell line. A cytotoxic drug was defined as one that promotes a decrease in confluence over time or a plateau in confluence with visual evidence of dead cells.

2.3. Western Blotting

ST88-14 cells (provided by George DeVries) were seeded at a density of 5000 per cm^2 of growth area on CellBind surfaces (Corning, NY, USA) and incubated at 37 °C, 5% CO_2. After approximately 96 h, medium was replaced with DMEM + 10% FBS containing 0.1% DMSO or 0.1 µM, 1 µM, and 10 µM of trametinib, mirdametinib, and selumetinib. After incubation for 30 min and 24 h, the cells were extracted in radioimmunoprecipitation (RIPA)

buffer (Cell Signaling, Danvers, MA, USA). Protein content was estimated using the detergent compatible (DC) protein assay by Bio-Rad (Hercules, CA, USA). Samples were loaded at 5 µg per lane in precast mini-PROTEAN gels (Bio-Rad, Hercules, CA, USA) for size separation, then transferred to 0.45 µm pore size PVDF Immobilon-FL transfer membranes (Millipore, Burlington, MA, USA). Membranes were blocked for 1 h in a 1:1 mixture of tris-buffered saline with 0.1% Tween 20 (TBS-T) and Odyssey blocking buffer (LI-COR Biosciences, Lincoln, NE, USA). Membranes where incubated with the following antibodies at indicated dilutions in 1:1 TBS-T/Odyssey blocking buffer overnight at 4 °C: rabbit anti-phospho-p44/42 MAPK (Erk1/2) (Thr202/Tyr204) (Cell Signaling #4370, 1:1000), mouse anti-p44/42 MAPK (Erk1/2) (Cell Signaling #4696, 1:500), and rabbit anti-alpha-tubulin (Cell Signaling #3873, 1:30,000). The next day, membranes were incubated with horseradish peroxidase-conjugated anti-rabbit IgG (Cell Signaling, 7074) and anti-mouse IgG (Cell Signaling, 7076) antibodies diluted to 1:5000 in TBS-T for 1 h at room temperature. Chemiluminescent blots were visualized using the SignalFire ECL Reagent (Cell Signaling, Danvers, MA, USA) and the Bio-Rad ChemiDoc MP Imaging System (Hercules, CA, USA).

2.4. Statistical Analysis

All high-content screens tested five or greater replicate wells per condition. Graphs and statistical analyses were generated using GraphPad Prism version 10.6.1. AUC calculations were performed using the area under the curve function, and dose–response curves were generated using the [inhibitor] vs. response variable slope function. Because GI50 values were distributed lognormally across nine orders of magnitude, the values for each drug were summarized using geometric means (i.e., averaging the Log10 values of GI50s in each MPNST cell line) with geometric standard deviation factors (GSDs) in place of standard errors. The geometric mean GI50s of trametinib, mirdametinib, and selumetinib were compared using a one-way, repeated-measures lognormal ANOVA with Geisser–Greenhouse correction and Tukey's multiple comparisons test.

3. Results

3.1. Trametinib and Fimepinostat Reduce MPNST Cell Confluence at Sub-Micromolar Doses

Table 2 summarizes the MPNST cell lines studied in high-content drug sensitivity assays. The characteristics of each cell line vary by location, NF1 status, and include primary tumors and metastases. The NMS-2 and NMS-2PC cell lines were derived from primary and metastatic lesions, respectively, from the same patient [41]. Notably, the STS-26T cell line was recently reclassified as a BRAF V600E mutant melanoma based on genomic analyses [45]. DMSO-treated MPNST cell lines reached near full confluence (>75%) in the 384-well format by 72 h of treatment (Figure 1A), except for NFS-1, which reached 65% confluence at the end of the five-day treatment period. Confluence curves for trametinib and fimepinostat-treated cells demonstrated dose-dependent decreases in well confluence over time across the nine cell lines (Figure 2). The GI50s in the nine MPNST cell lines were 17 nM for trametinib and 17 pM for fimepinostat, respectively. The GI50s in STS-26T melanoma cells were 0.45 µM for trametinib and 1.3 nM for fimepinostat, respectively (Table 3). The typical morphological effects of both drugs tested between 0.001 and 10 µM after 72 h of treatment in ST88-14 cells are shown (Figure 1B). Trametinib had cytotoxic effects at 0.1 µM, whereas fimepinostat had cytotoxic effects at 0.001 µM as evidenced by the presence of cellular debris during imaging (Figure 1B). Cytotoxic effects were observed in fimepinostat- and trametinib-treated cell lines except for NFS-1 and sNF02.2. These two cell lines underwent proliferation arrest with no substantial accumulation of cellular debris (Figure S1). Representative images of cell lines treated with their respective lowest cytotoxic dose of trametinib and fimepinostat are provided (Figures S2 and S3).

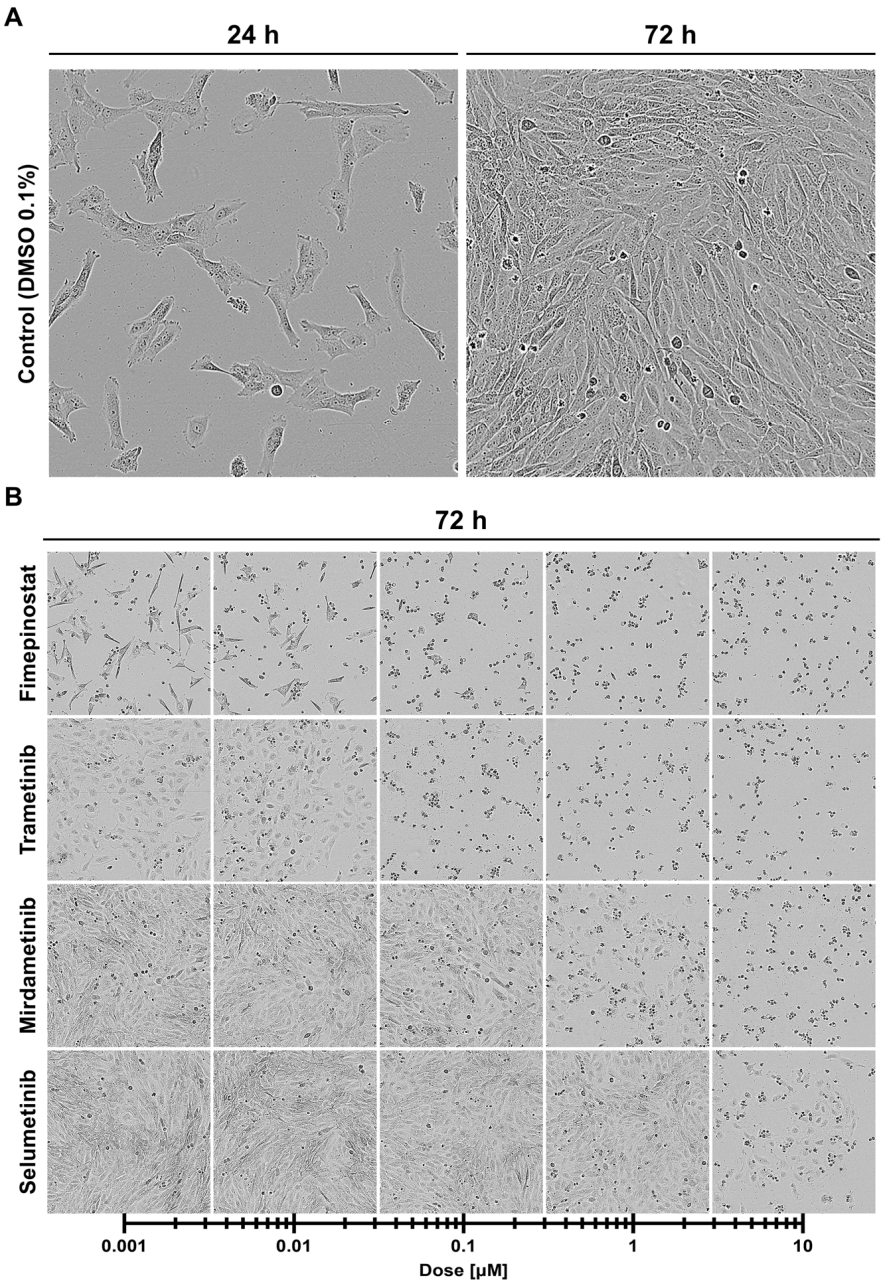


Figure 1. Trametinib and fimepinostat have cytotoxic effects on ST88-14 cells. The Incucyte system allows for timelapse imaging to determine drug effects on live cells. (**A**) Representative ST88-14 cell images captured during the high-content drug sensitivity assays at 24 h and 72 h of DMSO treatment. (**B**) Representative ST88-14 cell images captured at 72 h of indicated drug treatments. Fimepinostat promotes cytotoxicity by 72 h at all doses shown. Some surviving cells are observed with fimepinostat doses lower than 0.1 μM. Trametinib is more potent than mirdametinib and selumetinib. Substantial cell death is noted at 72 h of treatment with at least 0.1 μM trametinib. Cells treated with lower doses of trametinib reached near full confluence after 72 h of treatment.

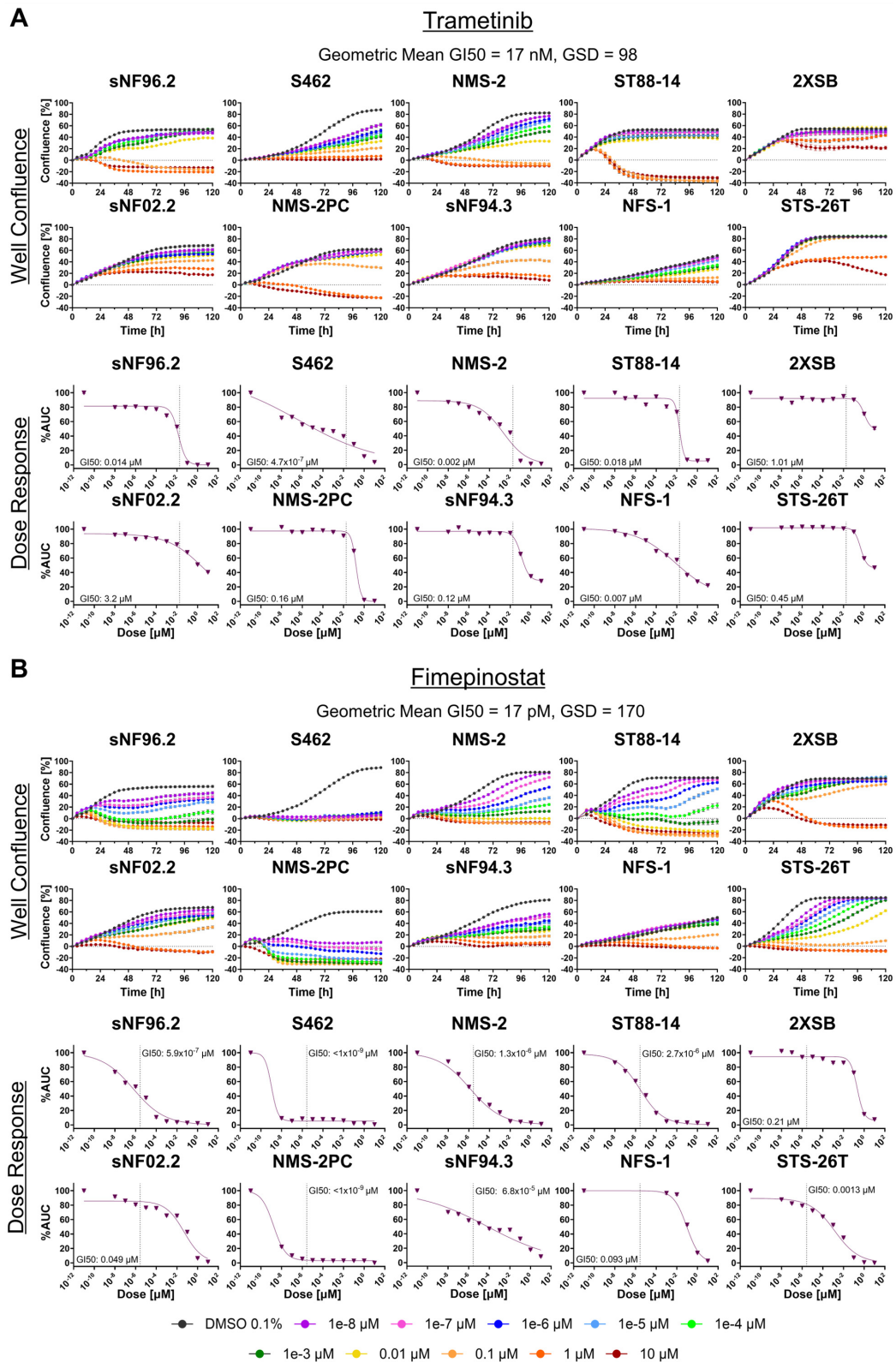


Figure 2. Trametinib and fimepinostat cause dose-dependent reductions in MPNST cell confluence over time. Confluence curves and AUC dose–response curves for (**A**) trametinib- and (**B**) fimepinostat-treated MPNST cells and the BRAF-V600E mutant melanoma cell line (STS-26T) reveal that both drugs promote dose-dependent reductions in cell confluence over time. Confluence is measured as a percentage of well area containing cells and normalized to confluence at treatment initiation. AUC dose–response curves were generated from confluence data for each cell line and normalized to DMSO-treated controls to calculate 50% growth inhibitory concentration (GI50) values. GSD = geometric standard deviation.

Table 3. GI50 values in all cell lines. Values were calculated based on the AUC of confluence curves generated during high-content screens (dosing range 10 μM to 10 fM).

Initial Assay		
Cell Line	Trametinib GI50 [μM]	Fimepinostat GI50 [μM]
sNF96.2 [1]	1.40×10^{-2}	5.90×10^{-7}
S462 [1]	4.70×10^{-7}	$<1.00 \times 10^{-9}$
NMS-2 [1,2]	2.10×10^{-3}	1.30×10^{-6}
ST88-14 [1]	1.80×10^{-2}	2.70×10^{-6}
2XSB	1.00×10^{0}	2.10×10^{-1}
sNF02.2	3.20×10^{0}	4.90×10^{-2}
NMS-2PC [2]	1.60×10^{-1}	$<1.00 \times 10^{-9}$
sNF94.3	1.20×10^{-1}	6.90×10^{-5}
NFS-1	7.40×10^{-3}	9.30×10^{-2}
Geometric Mean	1.70×10^{-3}	1.70×10^{-5}
GSD	9.80×10^{1}	1.70×10^{3}
STS-26T [1,3]	4.50×10^{-1}	1.30×10^{-3}

Comparative MEK Inhibitor Assay			
Cell Line	Trametinib GI50 [μM]	Mirdametinib GI50 [μM]	Selumetinib GI50 [μM]
2XSB	1.00×10^{0}	6.40×10^{0}	1.00×10^{1}
ST88-14	1.80×10^{-2}	7.70×10^{-1}	4.20×10^{0}
NMS-2PC	3.70×10^{-2}	1.40×10^{0}	8.20×10^{0}
NMS-2	7.60×10^{-3}	9.10×10^{-1}	1.70×10^{0}
Geometric Mean	4.76×10^{-2}	1.58×10^{0}	4.92×10^{0}
GSD	8.5	2.6	2.2

[1] Cell lines with known altered PTEN status. [2] Cell lines were isolated from two distinct tumors resected from the same patient. [3] Reclassified as BRAF V600E-mutant melanoma, originally classified as a sporadic MPNST.

3.2. Trametinib Is More Potent than Mirdametinib and Selumetinib

To directly compare the efficacies of trametinib with mirdametinib and selumetinib, we treated a subset of four MPNST cell lines with the three MEK inhibitors. Representative cell lines for neurofibromin protein status, primary vs. metastatic status, and a range of GI50s from the initial trametinib screens were selected for comparison (2XSB, ST88-14, NMS-2, NMS-2PC). Specifically, 2XSB was the only sporadic MPNST cell line screened in this study [43]; all other MPNST cell lines were isolated from NF1 patient tumors. In these four cell lines, trametinib had a lower geometric mean GI50 (48 nM) compared to mirdametinib (1.6 μM, $p = 0.021$) and selumetinib (4.9 μM, $p = 0.019$; Figure 3B,C). Trametinib treatment for 72 h induced ST88-14 cytotoxicity at doses as low as 0.1 μM (Figure 1B). Mirdametinib treatment for 72 h induced cytotoxicity in ST88-14 cells as low as 1 μM; selumetinib treatment for 72 h induced cytotoxicity only at the maximum dose tested (10 μM; Figure 1B). Doses of trametinib (0.1, 1, and 10 μM), mirdametinib (1 and 10 μM), and selumetinib (10 μM) that promoted ST88-14 cell death demonstrated sustained inhibition of ERK T202/Y204 phosphorylation (pERK) upon Western blotting through 24 h of treatment (Figure 3D). Doses of mirdametinib (0.1 μM) and selumetinib (0.1 and 1 μM) that failed to promote ST88-14 cell death failed to inhibit pERK at 24 h of treatment. Some ineffective doses of mirdametinib (0.1 μM) and selumetinib (1 μM) inhibited pERK at 30 min but not at 24 h of treatment.

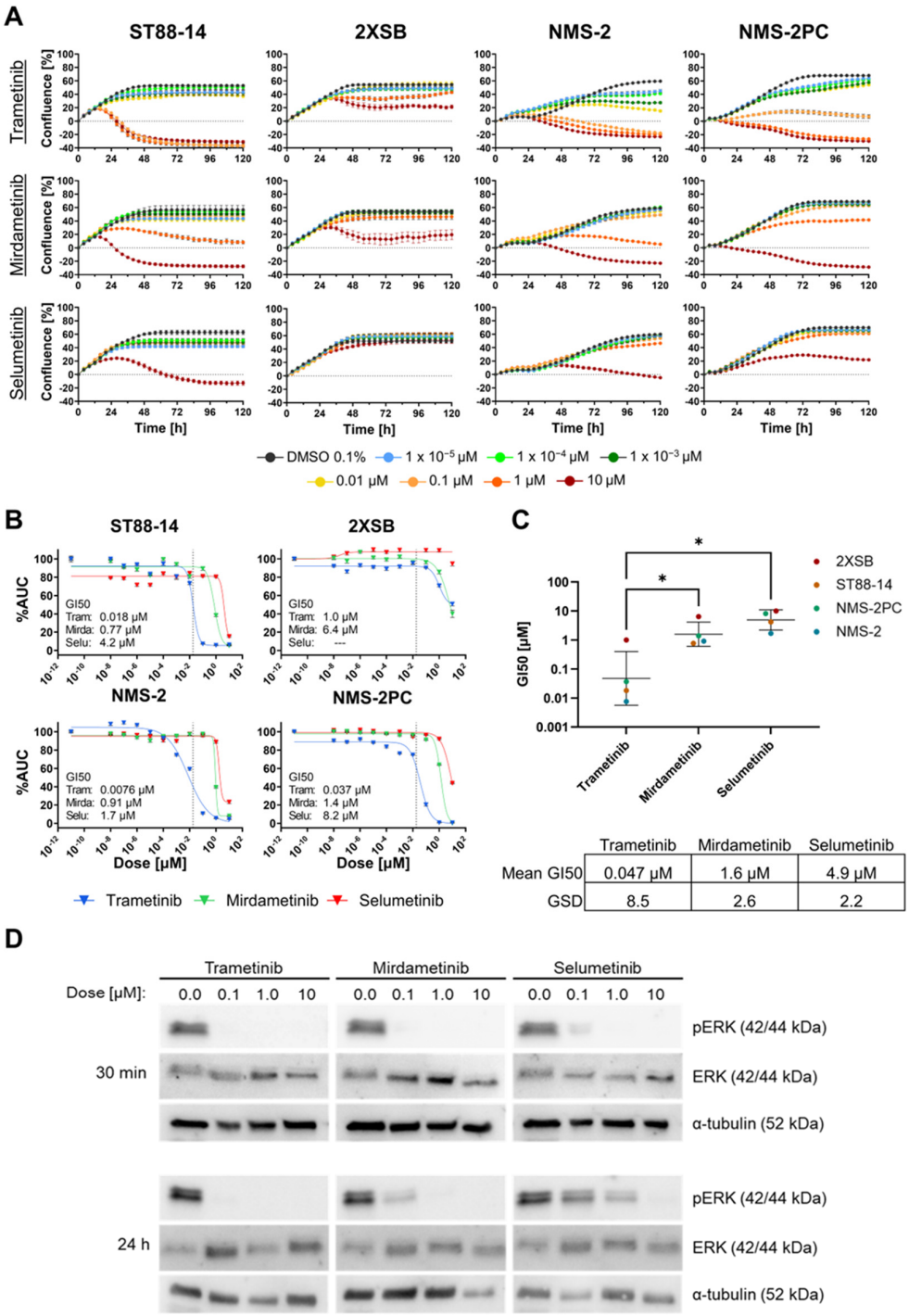


Figure 3. Trametinib is a more potent MEK inhibitor in MPNST cells than mirdametinib and selumetinib. Three MEK inhibitors were compared in four MPNST cell lines using the high-content drug sensitivity assay. Trametinib had lower GI50s than mirdametinib and selumetinib in all cell lines. (**A**) Confluence curves for trametinib, mirdametinib, and selumetinib in four MPNST cell lines. Confluence is measured as percentage of well area containing cells and normalized to confluence at treatment initiation. (**B**) AUC curves generated from confluence data in the four cell lines (normalized to DMSO-treated controls). (**C**) Geometric mean 50% growth inhibitory concentrations (GI50) values for trametinib, mirdametinib, and selumetinib in each cell line tested. Error bars represent the geometric standard deviation (GSD). (**D**) Western blots for pERK, total ERK, and α-tubulin loading controls in ST88-14 cells after treatment with indicated MEK inhibitors for 30 min and 24 h. The original images of the Western Blotting figures can be found in Supplementary Data.

4. Discussion

Clinical trials for small molecule inhibitors in MPNSTs have been disappointing. Two trials reported a 0% objective response rate or progressive disease for NF1-related tumors [46,47]. The SARC006 clinical trial which established the current standard of care for unresectable MPNSTs evaluated traditional chemotherapeutics in cycles of ifosfamide/doxorubicin and ifosfamide/etoposide. However, this regimen promoted a partial response in only 5/28 MPNST patients with NF1 [48]. Planned and recruiting clinical trials will evaluate selumetinib alone and in combination with an MDM2 inhibitor and mirdametinib in combination with the pan-HDAC inhibitor vorinostat (NCT06735820, NCT05253131, NCT06693284). A complete sustained clinical response to trametinib lasting over 15 months was reported for a pediatric case of recurrent metastatic MPNST with biallelic *NF1* deletion [33], suggesting that trametinib is a strong candidate for larger clinical trials.

Recent preclinical studies identified both trametinib and HDAC inhibitors as potential therapeutics for MPNSTs. Two large *in vitro* screening campaigns using up to seven patient MPNST cell lines with single time point measurements indicated that HDAC inhibitors reduced cell viability at 48 or 72 h of treatment [34,35]. Others demonstrated that HDAC inhibition with abexinostat (PCI-2478) triggered apoptosis in four sensitive patient MPNST cell lines including ST88-14, S462, and two others not tested here [49]. A targeted preclinical study also used single timepoint assays in four patient MPNST cell lines to demonstrate that trametinib was more potent than other MEK inhibitors including selumetinib and mirdametinib [30]. The combination of MEK, BET, and CDK inhibitors has also recently demonstrated preclinical efficacy for MPNSTs [50].

This focused preclinical study used high-content imaging to track well confluence over 120 h of treatment in nine patient-derived MPNST lines. We found that trametinib is 30- and 100-fold more potent than the FDA-approved NF1 MEK inhibitors mirdametinib and selumetinib. Western blots revealed that trametinib was superior to selumetinib and mirdametinib in its ability to sustain MEK inhibition at lower doses for 24 h as measured by pERK levels in ST88-14 cells. Doses of the drugs that inhibited MEK for 24 h were associated with ST88-14 cell death. ST88-14 cell death was not detected in cultures treated with doses of mirdametinib and selumetinib that did not inhibit MEK for 24 h. X-ray crystallography studies have shown that trametinib binds the kinase suppressor of Ras (KSR) scaffold needed for MEK activation rather than blocking th e ATP-binding region of MEK, as do selumetinib and mirdametinib [51]. This could explain the observed enhanced MEK inhibitory capacity of trametinib compared to other MEK inhibitors in both MPNST and schwannoma cells [31,32]. Trametinib is FDA-approved for BRAF-mutant melanomas alone and in combination with dabrafenib (Tafinlar). Notably, trametinib was more potent in 8/9 MPNST cell lines than in the BRAF-mutant STS-26T melanoma cell line [45]. In BRAF-mutant melanomas, trametinib improves progression-free and overall survival compared to traditional chemotherapies with an acceptable tolerability profile [52]. The most common reported dose-limiting adverse effects of trametinib include rash, fatigue, and hypertension [53]. This evidence, taken together with promising results from a precision medicine case study [33], supports potential clinical trials investigating trametinib for the treatment of MPNSTs.

The high-content assays in this study revealed that the dual HDAC/PI3K inhibitor fimepinostat triggers MPNST cell death at picomolar concentrations. HDACs primarily function as epigenetic regulators by deacetylating lysine residues on histone tails and promoting chromatin condensation [54]. Thus, HDACs are vulnerable targets in cancer cells with dysregulated anti-tumor signaling pathways. HDAC inhibitors have been studied as therapeutic agents for cancer, cardiovascular diseases, and neurological diseases, and FDA-

approved HDAC inhibitors exist for aggressive cervical, brain, breast, and liver cancers among others [54,55]. HDAC inhibitors are under clinical investigation in combination with other anti-cancer therapies [56,57]. MPNSTs express class I HDAC enzymes, namely HDAC1 and HDAC8; targeting either isoform promotes cell death in MPNST cells [58–60]. HDAC8 can reside in both the nucleus and cytoplasm where it regulates acetylation of non-histone proteins [54,58,61]. However, exclusively targeting nuclear HDACs with HDAC1/2 specific inhibitors also results in MPNST cell death [49], suggesting nuclear HDAC function plays a critical role in MPNST cell survival. Fimepinostat is a potent inhibitor of class I HDACs in cell-free assays with IC50s for HDAC1, HDAC2, and HDAC8 of 1.7 nM, 5.0 nM, and 191 nM, respectively [62]. Fimepinostat also promotes cell death in human schwannoma cells, whereas vorinostat does not [37]. The most common dose-limiting adverse effects of fimepinostat are gastrointestinal and hematologic disturbances [63,64].

The dual PI3K inhibitory function of fimepinostat positions it as a strong candidate therapeutic for MPNSTs with PTEN loss. PI3K activity is frequently increased in MPNSTs due to PTEN loss [20,65]. Alterations in PTEN gene dosage have been reported in up to 58% of MPNSTs [40], and PTEN loss is correlated with poorer survival outcomes [66]. This suggests that, by targeting both HDACs and PI3K, fimepinostat could be beneficial for treating MPNSTs with altered PTEN expression. Fimepinostat targets PI3K subunits α, β, δ, and γ with IC50s of 19 nM, 54 nM, 39 nM, and 311 nM, respectively [62]. Four of the five most sensitive cell lines have reported altered PTEN status [45]. Fimepinostat had sub-picomolar GI50s in each of the four PTEN-altered MPNST cell lines. The predictive potential for PTEN loss as a therapeutic MPNST biomarker warrants further investigation.

5. Conclusions

These results support further clinical investigation of trametinib and fimepinostat as alternatives to the standards of care for MPNSTs. By extension, the evidence provided here suggests that trametinib and fimepinostat monotherapies could be more efficacious in MPNST patients than combinations using selumetinib (NCT06735820, NCT05253131) or mirdametinib (NCT06693284).

Supplementary Materials: The following supporting information can be downloaded at https://www.mdpi.com/article/10.3390/cancers18050746/s1, Figure S1: Cytostatic effects of trametinib in sNF02.2 and NFS-1 cell lines; Figure S2: Lowest effective doses of trametinib in all cell lines; Figure S3: Lowest effective doses of fimepinostat in all cell lines; Supplementary Data: Western blot raw images.

Author Contributions: E.W.H.: conceptualization, methodology, formal analysis, investigation, writing—original draft, review and editing, funding acquisition. S.A.O.: investigation, writing—review and editing. C.F.-V.: supervision, project administration, conceptualization, investigation, writing—original draft, review and editing, funding acquisition. All authors have read and agreed to the published version of the manuscript.

Funding: This work was funded by the NIH/NIDCD R01DC017264 award to C.F.V. and the University of Central Florida College of Medicine MD/PhD Scholarship award to E.W.H.

Institutional Review Board Statement: The use of de-identified human MPNST cell lines in this study has been deemed non-human subjects research by the University of Central Florida Institutional Review Board.

Data Availability Statement: The raw data supporting the conclusions of this article will be made available by the authors on request.

Acknowledgments: The authors would like to thank Steven Carroll, Jody Longo, George DeVries, and Margaret Wallace for providing the cell lines used in this study.

Conflicts of Interest: The authors declare no conflicts of interest.

Abbreviations

The following abbreviations are used in this manuscript:

ANNUBP	atypical neurofibromatous neoplasm with uncertain biologic potential
AUC	area under the curve
DMEM	Dulbecco's modified eagle medium
FBS	fetal bovine serum
GI50	50% growth inhibitory dose
GSD	geometric standard deviation
HDAC	histone deacetylase
MEK	mitogen-activated protein kinase kinase
MPNST	malignant peripheral nerve sheath tumor
NF1	Neurofibromatosis type 1
PI3K	phosphoinositide-3-kinase
pNF	plexiform neurofibroma

References

1. Wallace, M.R.; Marchuk, D.A.; Andersen, L.B.; Letcher, R.; Odeh, H.M.; Saulino, A.M.; Fountain, J.W.; Brereton, A.; Nicholson, J.; Mitchell, A.L.; et al. Type 1 Neurofibromatosis Gene: Identification of a Large Transcript Disrupted in Three NF1 Patients. *Science* **1990**, *249*, 181–186. [CrossRef]
2. Lee, T.S.J.; Chopra, M.; Kim, R.H.; Parkin, P.C.; Barnett-Tapia, C. Incidence and Prevalence of Neurofibromatosis Type 1 and 2: A Systematic Review and Meta-Analysis. *Orphanet J. Rare Dis.* **2023**, *18*, 292. [CrossRef]
3. Kresak, J.L.; Walsh, M. Neurofibromatosis: A Review of NF1, NF2, and Schwannomatosis. *J. Pediatr. Genet.* **2016**, *5*, 98. [CrossRef]
4. Gutmann, D.H.; Ferner, R.E.; Listernick, R.H.; Korf, B.R.; Wolters, P.L.; Johnson, K.J. Neurofibromatosis Type 1. *Nat. Rev. Dis. Primers* **2017**, *3*, 17004. [CrossRef]
5. Belakhoua, S.M.; Rodriguez, F.J. Diagnostic Pathology of Tumors of Peripheral Nerve. *Neurosurgery* **2021**, *88*, 443. [CrossRef]
6. Evans, D.G.R.; Baser, M.E.; McGaughran, J.; Sharif, S.; Howard, E.; Moran, A. Malignant Peripheral Nerve Sheath Tumours in Neurofibromatosis 1. *J. Med. Genet.* **2002**, *39*, 311–314. [CrossRef]
7. McCaughan, J.A.; Holloway, S.M.; Davidson, R.; Lam, W.W.K. Further Evidence of the Increased Risk for Malignant Peripheral Nerve Sheath Tumour from a Scottish Cohort of Patients with Neurofibromatosis Type 1. *J. Med. Genet.* **2007**, *44*, 463–466. [CrossRef] [PubMed]
8. Hirbe, A.C.; Gutmann, D.H. Neurofibromatosis Type 1: A Multidisciplinary Approach to Care. *Lancet Neurol.* **2014**, *13*, 834–843. [CrossRef]
9. De Raedt, T.; Brems, H.; Wolkenstein, P.; Vidaud, D.; Pilotti, S.; Perrone, F.; Mautner, V.; Frahm, S.; Sciot, R.; Legius, E. Elevated Risk for MPNST in NF1 Microdeletion Patients. *Am. J. Hum. Genet.* **2003**, *72*, 1288. [CrossRef] [PubMed]
10. Koczkowska, M.; Chen, Y.; Callens, T.; Gomes, A.; Sharp, A.; Johnson, S.; Hsiao, M.C.; Chen, Z.; Balasubramanian, M.; Barnett, C.P.; et al. Genotype-Phenotype Correlation in NF1: Evidence for a More Severe Phenotype Associated with Missense Mutations Affecting NF1 Codons 844–848. *Am. J. Hum. Genet.* **2017**, *102*, 69. [CrossRef] [PubMed]
11. Pourtsidis, A.; Doganis, D.; Baka, M.; Bouhoutsou, D.; Varvoutsi, M.; Synodinou, M.; Giamarelou, P.; Kosmidis, H. Malignant Peripheral Nerve Sheath Tumors in Children with Neurofibromatosis Type 1. *Case Rep. Oncol. Med.* **2014**, *2014*, 843749. [CrossRef]
12. Peltonen, S.; Kallionpää, R.A.; Rantanen, M.; Uusitalo, E.; Lähteenmäki, P.M.; Pöyhönen, M.; Pitkäniemi, J.; Peltonen, J. Pediatric Malignancies in Neurofibromatosis Type 1: A Population-Based Cohort Study. *Int. J. Cancer* **2019**, *145*, 2926–2932. [CrossRef]
13. Kehrer-Sawatzki, H.; Kluwe, L.; Salamon, J.; Well, L.; Farschtschi, S.; Rosenbaum, T.; Mautner, V.F. Clinical Characterization of Children and Adolescents with NF1 Microdeletions. *Child's Nerv. Syst.* **2020**, *36*, 2297. [CrossRef]
14. Watson, K.L.; Al Sannaa, G.A.; Kivlin, C.M.; Ingram, D.R.; Landers, S.M.; Roland, C.L.; Cormier, J.N.; Hunt, K.K.; Feig, B.W.; Guadagnolo, B.A.; et al. Patterns of Recurrence and Survival in Sporadic, Neurofibromatosis Type 1–Associated, and Radiation-Associated Malignant Peripheral Nerve Sheath Tumors. *J. Neurosurg.* **2017**, *126*, 319–329. [CrossRef]
15. Hirbe, A.C.; Dehner, C.A.; Dombi, E.; Eulo, V.; Gross, A.M.; Sundby, T.; Lazar, A.J.; Widemann, B.C. Contemporary Approach to Neurofibromatosis Type 1–Associated Malignant Peripheral Nerve Sheath Tumors. *Am. Soc. Clin. Oncol. Educ. Book* **2024**, *44*, e432242. [CrossRef]
16. Yu, Y.; Wei, C.; Yue, M.; Zhang, C.; Wang, Y.; Wang, Z. From Benign Neurofibromas to Malignant Peripheral Nerve Sheath Tumors (MPNST): A Gaming among Multiple Factors. *Cell. Oncol.* **2025**, *48*, 841. [CrossRef]

17. Lee, W.; Teckie, S.; Wiesner, T.; Ran, L.; Prieto Granada, C.N.; Lin, M.; Zhu, S.; Cao, Z.; Liang, Y.; Sboner, A.; et al. PRC2 Is Recurrently Inactivated through EED or SUZ12 Loss in Malignant Peripheral Nerve Sheath Tumors. *Nat. Genet.* **2014**, *46*, 1227–1232. [CrossRef]
18. Zhang, M.; Wang, Y.; Jones, S.; Sausen, M.; McMahon, K.; Sharma, R.; Wang, Q.; Belzberg, A.J.; Chaichana, K.; Gallia, G.L.; et al. Somatic Mutations of SUZ12 in Malignant Peripheral Nerve Sheath Tumors. *Nat. Genet.* **2014**, *46*, 1170–1172. [CrossRef] [PubMed]
19. Carroll, S.L. Molecular Mechanisms Promoting the Pathogenesis of Schwann Cell Neoplasms. *Acta Neuropathol.* **2011**, *123*, 321. [CrossRef] [PubMed]
20. Bradtmöller, M.; Hartmann, C.; Zietsch, J.; Jäschke, S.; Mautner, V.F.; Kurtz, A.; Park, S.J.; Baier, M.; Harder, A.; Reuss, D.; et al. Impaired Pten Expression in Human Malignant Peripheral Nerve Sheath Tumours. *PLoS ONE* **2012**, *7*, e47595. [CrossRef] [PubMed]
21. Lemberg, K.M.; Wang, J.; Pratilas, C.A. From Genes to -Omics: The Evolving Molecular Landscape of Malignant Peripheral Nerve Sheath Tumor. *Genes* **2020**, *11*, 691. [CrossRef] [PubMed]
22. Somaiah, N.; Paudyal, B.; Winkler, R.E.; Van Tine, B.A.; Hirbe, A.C. Malignant Peripheral Nerve Sheath Tumor, a Heterogeneous, Aggressive Cancer with Diverse Biomarkers and No Targeted Standard of Care: Review of the Literature and Ongoing Investigational Agents. *Target. Oncol.* **2024**, *19*, 665. [CrossRef] [PubMed]
23. Suppiah, S.; Mansouri, S.; Mamatjan, Y.; Liu, J.C.; Bhunia, M.M.; Patil, V.; Rath, P.; Mehani, B.; Heir, P.; Bunda, S.; et al. Multiplatform Molecular Profiling Uncovers Two Subgroups of Malignant Peripheral Nerve Sheath Tumors with Distinct Therapeutic Vulnerabilities. *Nat. Commun.* **2023**, *14*, 2696. [CrossRef] [PubMed]
24. Lucas, C.H.G.; Vasudevan, H.N.; Chen, W.C.; Magill, S.T.; Braunstein, S.E.; Jacques, L.; Dahiya, S.; Rodriguez, F.J.; Horvai, A.E.; Perry, A.; et al. Histopathologic Findings in Malignant Peripheral Nerve Sheath Tumor Predict Response to Radiotherapy and Overall Survival. *Neurooncol. Adv.* **2020**, *2*, vdaa131. [CrossRef]
25. Porter, D.E.; Prasad, V.; Foster, L.; Dall, G.F.; Birch, R.; Grimer, R.J. Survival in Malignant Peripheral Nerve Sheath Tumours: A Comparison between Sporadic and Neurofibromatosis Type 1-Associated Tumours. *Sarcoma* **2009**, *2009*, 756395. [CrossRef]
26. Widemann, B.C. Current Status of Sporadic and Neurofibromatosis Type 1–Associated Malignant Peripheral Nerve Sheath Tumors. *Curr. Oncol. Rep.* **2009**, *11*, 322. [CrossRef]
27. Martin, E.; Coert, J.H.; Flucke, U.E.; Slooff, W.B.M.; Ho, V.K.Y.; van der Graaf, W.T.; van Dalen, T.; van de Sande, M.A.J.; van Houdt, W.J.; Grünhagen, D.J.; et al. A Nationwide Cohort Study on Treatment and Survival in Patients with Malignant Peripheral Nerve Sheath Tumours. *Eur. J. Cancer* **2020**, *124*, 77–87. [CrossRef]
28. Jansma, C.Y.M.N.; Acem, I.; Grünhagen, D.J.; Verhoef, C.; Martin, E.; Coert, J.H.; Flucke, U.E.; Slooff, W.B.M.; Van Dalen, T.; Been, L.B.; et al. Local Recurrence in Malignant Peripheral Nerve Sheath Tumours: Multicentre Cohort Study. *BJS Open* **2024**, *8*, zrae024. [CrossRef]
29. Kahn, J.; Gillespie, A.; Tsokos, M.; Ondos, J.; Dombi, E.; Camphausen, K.; Widemann, B.C.; Kaushal, A. Radiation Therapy in Management of Sporadic and Neurofibromatosis Type 1-Associated Malignant Peripheral Nerve Sheath Tumors. *Front. Oncol.* **2014**, *4*, 324. [CrossRef]
30. Gu, Y.; Wang, W.; Li, Y.; Li, H.; Guo, Z.; Wei, C.; Long, M.; Chung, M.; Aimaier, R.; Li, Q.; et al. Preclinical Assessment of MEK Inhibitors for Malignant Peripheral Nerve Sheath Tumors Reveals Differences in Efficacy and Adaptive Response. *Front. Oncol.* **2022**, *12*, 903177. [CrossRef]
31. Fuse, M.A.; Dinh, C.T.; Vitte, J.; Kirkpatrick, J.; Mindos, T.; Plati, S.K.; Young, J.I.; Huang, J.; Carlstedt, A.; Franco, M.C.; et al. Preclinical Assessment of MEK1/2 Inhibitors for Neurofibromatosis Type 2-Associated Schwannomas Reveals Differences in Efficacy and Drug Resistance Development. *Neuro. Oncol.* **2019**, *21*, 486–497. [CrossRef]
32. Hardin, H.M.; Hass, E.W.; Allaway, R.; Morrison, H.; Fernandez-Valle, C. BET Proteins Mediate Survival Mechanisms in Human Schwannoma Model Cells Challenged with Trametinib but Not Brigatinib. *Oncogene* **2025**, *44*, 4699–4711. [CrossRef]
33. Nagabushan, S.; Lau, L.M.S.; Barahona, P.; Wong, M.; Sherstyuk, A.; Marshall, G.M.; Tyrrell, V.; Wegner, E.A.; Ekert, P.G.; Cowley, M.J.; et al. Efficacy of MEK Inhibition in a Recurrent Malignant Peripheral Nerve Sheath Tumor. *npj Precis. Oncol.* **2021**, *5*, 9. [CrossRef]
34. Guo, J.; Grovola, M.R.; Xie, H.; Coggins, G.E.; Duggan, P.; Hasan, R.; Huang, J.; Lin, D.W.; Song, C.; Witek, G.M.; et al. Comprehensive Pharmacological Profiling of Neurofibromatosis Cell Lines. *Am. J. Cancer Res.* **2017**, *7*, 923.
35. Fernández-Rodríguez, J.; Creus-Bachiller, E.; Zhang, X.; Martínez-Iniesta, M.; Ortega-Bertran, S.; Guha, R.; Thomas, C.J.; Wallace, M.R.; Romagosa, C.; Salazar-Huayna, L.; et al. A High-Throughput Screening Platform Identifies Novel Combination Treatments for Malignant Peripheral Nerve Sheath Tumors. *Mol. Cancer Ther.* **2022**, *21*, 1246. [CrossRef]
36. Huegel, J.; Dinh, C.T.; Martinelli, M.; Bracho, O.; Rosario, R.; Hardin, H.; Estivill, M.; Griswold, A.; Gultekin, S.; Liu, X.Z.; et al. CUDC907, a Dual Phosphoinositide-3 Kinase/Histone Deacetylase Inhibitor, Promotes Apoptosis of NF2 Schwannoma Cells. *Oncotarget* **2022**, *13*, 890–904. [CrossRef] [PubMed]

37. Allaway, R.; Angus, S.P.; Beauchamp, R.L.; Blakeley, J.O.; Bott, M.; Burns, S.S.; Carlstedt, A.; Chang, L.S.; Chen, X.; Clapp, D.W.; et al. Traditional and Systems Biology Based Drug Discovery for the Rare Tumor Syndrome Neurofibromatosis Type 2. *PLoS ONE* **2018**, *13*, e0197350. [CrossRef]
38. Muir, D.; Neubauer, D.; Lim, I.T.; Yachnis, A.T.; Wallace, M.R. Tumorigenic Properties of Neurofibromin-Deficient Neurofibroma Schwann Cells. *Am. J. Pathol.* **2001**, *158*, 501–513. [CrossRef] [PubMed]
39. Perrin, G.Q.; Li, H.; Fishbein, L.; Thomson, S.A.; Hwang, M.S.; Scarborough, M.T.; Yachnis, A.T.; Wallace, M.R.; Mareci, T.H.; Muir, D. An Orthotopic Xenograft Model of Intraneural NF1 MPNST Suggests a Potential Association between Steroid Hormones and Tumor Cell Proliferation. *Lab. Investig.* **2007**, *87*, 1092–1102. [CrossRef]
40. Holtkamp, N.; Malzer, E.; Zietsch, J.; Okuducu, A.F.; Mucha, J.; Mawrin, C.; Mautner, V.F.; Schildhaus, H.U.; Von Deimling, A. EGFR and ErbB2 in Malignant Peripheral Nerve Sheath Tumors and Implications for Targeted Therapy. *Neuro Oncol.* **2008**, *10*, 946. [CrossRef] [PubMed]
41. Imaizumi, S.; Motoyama, T.; Ogose, A.; Hotta, T.; Takahashi, H.E. Characterization and Chemosensitivity of Two Human Malignant Peripheral Nerve Sheath Tumour Cell Lines Derived from a Patient with Neurofibromatosis Type 1. *Virchows Arch.* **1998**, *433*, 435–441. [CrossRef]
42. Fletcher, J.A.; Kozakewich, H.P.; Hoffer, F.A.; Lage, J.M.; Weidner, N.; Tepper, R.; Pinkus, G.S.; Morton, C.C.; Corson, J.M. Diagnostic Relevance of Clonal Cytogenetic Aberrations in Malignant Soft-Tissue Tumors. *N. Engl. J. Med.* **1991**, *324*, 436–443. [CrossRef]
43. Longo, J.F.; Brosius, S.N.; Znoyko, I.; Alers, V.A.; Jenkins, D.P.; Wilson, R.C.; Carroll, A.J.; Wolff, D.J.; Roth, K.A.; Carroll, S.L. Establishment and Genomic Characterization of a Sporadic Malignant Peripheral Nerve Sheath Tumor Cell Line. *Sci. Rep.* **2021**, *11*, 5690. [CrossRef]
44. Dahlberg, W.K.; Little, J.B.; Fletcher, J.A.; Suit, H.D.; Okunieff, P. Radiosensitivity in Vitro of Human Soft Tissue Sarcoma Cell Lines and Skin Fibroblasts Derived from the Same Patients. *Int. J. Radiat. Biol.* **1993**, *63*, 191–198. [CrossRef]
45. Magallón-Lorenz, M.; Terribas, E.; Ortega-Bertran, S.; Creus-Bachiller, E.; Fernández, M.; Requena, G.; Rosas, I.; Mazuelas, H.; Uriarte-Arrazola, I.; Negro, A.; et al. Deep Genomic Analysis of Malignant Peripheral Nerve Sheath Tumor Cell Lines Challenges Current Malignant Peripheral Nerve Sheath Tumor Diagnosis. *iScience* **2023**, *26*, 106096. [CrossRef] [PubMed]
46. Kim, A.; Lu, Y.; Okuno, S.H.; Reinke, D.; Maertens, O.; Perentesis, J.; Basu, M.; Wolters, P.L.; De Raedt, T.; Chawla, S.; et al. Targeting Refractory Sarcomas and Malignant Peripheral Nerve Sheath Tumors in a Phase I/II Study of Sirolimus in Combination with Ganetespib (SARC023). *Sarcoma* **2020**, *2020*, 5784876. [CrossRef]
47. Albritton, K.H.; Rankin, C.; Coffin, C.M.; Ratner, N.; Budd, G.T.; Schuetze, S.M.; Randall, R.L.; Declue, J.E.; Borden, E.C. Phase II Study of Erlotinib in Metastatic or Unresectable Malignant Peripheral Nerve Sheath Tumors (MPNST). *J. Clin. Oncol.* **2006**, *24*, 9518. [CrossRef]
48. Higham, C.S.; Steinberg, S.M.; Dombi, E.; Perry, A.; Helman, L.J.; Schuetze, S.M.; Ludwig, J.A.; Staddon, A.; Milhem, M.M.; Rushing, D.; et al. SARC006: Phase II Trial of Chemotherapy in Sporadic and Neurofibromatosis Type 1 Associated Chemotherapy-Naive Malignant Peripheral Nerve Sheath Tumors. *Sarcoma* **2017**, *2017*, 8685638. [CrossRef] [PubMed]
49. Lopez, G.; Torres, K.; Liu, J.; Hernandez, B.; Young, E.; Belousov, R.; Bolshakov, S.; Lazar, A.J.; Slopis, J.M.; McCutcheon, I.E.; et al. Autophagic Survival in Resistance to Histone Deacetylase Inhibitors: Novel Strategies to Treat Malignant Peripheral Nerve Sheath Tumors. *Cancer Res.* **2010**, *71*, 185. [CrossRef]
50. Ortega-Bertran, S.; Fernández-Rodríguez, J.; Magallón-Lorenz, M.; Zhang, X.; Creus-Bachiller, E.; Diazgranados, A.P.; Uriarte-Arrazola, I.; Mazuelas, H.; Blanco, I.; Valverde, C.; et al. Triple Combination of MEK, BET, and CDK Inhibitors Significantly Reduces Human Malignant Peripheral Nerve Sheath Tumors in Mouse Models. *Clin. Cancer Res.* **2025**, *31*, 907–920. [CrossRef]
51. Khan, Z.M.; Real, A.M.; Marsiglia, W.M.; Chow, A.; Duffy, M.E.; Yerabolu, J.R.; Scopton, A.P.; Dar, A.C. Structural Basis for the Action of the Drug Trametinib at KSR-Bound MEK. *Nature* **2020**, *588*, 509. [CrossRef]
52. Flaherty, K.T.; Robert, C.; Hersey, P.; Nathan, P.; Garbe, C.; Milhem, M.; Demidov, L.V.; Hassel, J.C.; Rutkowski, P.; Mohr, P.; et al. Improved Survival with MEK Inhibition in BRAF-Mutated Melanoma. *N. Engl. J. Med.* **2012**, *367*, 107–114. [CrossRef]
53. Hoffner, B.; Benchich, K. Trametinib: A Targeted Therapy in Metastatic Melanoma. *J. Adv. Pract. Oncol.* **2018**, *9*, 741. [CrossRef]
54. Yudaev, P.; Aleksandrova, Y.; Neganova, M. Recent Insights into the Creation of Histone Deacetylase Inhibitors for the Treatment of Human Diseases. *Int. J. Mol. Sci.* **2025**, *26*, 8629. [CrossRef]
55. Parveen, R.; Harihar, D.; Chatterji, B.P. Recent Histone Deacetylase Inhibitors in Cancer Therapy. *Cancer* **2023**, *129*, 3372–3380. [CrossRef]
56. Zhou, M.; Yuan, M.; Zhang, M.; Lei, C.; Aras, O.; Zhang, X.; An, F. Combining Histone Deacetylase Inhibitors (HDACis) with Other Therapies for Cancer Therapy. *Eur. J. Med. Chem.* **2021**, *226*, 113825. [CrossRef] [PubMed]
57. Suraweera, A.; O'Byrne, K.J.; Richard, D.J. Combination Therapy with Histone Deacetylase Inhibitors (HDACi) for the Treatment of Cancer: Achieving the Full Therapeutic Potential of HDACi. *Front. Oncol.* **2018**, *8*, 351964. [CrossRef]

58. Lopez, G.; Bill, K.L.J.; Bid, H.K.; Braggio, D.; Constantino, D.; Prudner, B.; Zewdu, A.; Batte, K.; Lev, D.; Pollock, R.E. HDAC8, A Potential Therapeutic Target for the Treatment of Malignant Peripheral Nerve Sheath Tumors (MPNST). *PLoS ONE* **2015**, *10*, e0133302. [CrossRef] [PubMed]
59. Lopez, G.; Pollock, R.E. Evaluating the Effect of HDAC8 Inhibition in Malignant Peripheral Nerve Sheath Tumors. In *HDAC/HAT Function Assessment and Inhibitor Development*; Methods in Molecular Biology; Humana: New York, NY, USA, 2017; Volume 1510, pp. 365–374. [CrossRef]
60. Soukar, I.; Fisher, R.J.; Bhagavatula, S.; Collard, M.; Cole, P.A.; Alani, R.M. The CoREST Complex Is a Therapeutic Vulnerability in Malignant Peripheral Nerve Sheath Tumors. *Sci. Rep.* **2025**, *15*, 10128. [CrossRef] [PubMed]
61. Singh, B.N.; Zhang, G.; Hwa, Y.L.; Li, J.; Dowdy, S.C.; Jiang, S.W. Nonhistone Protein Acetylation as Cancer Therapy Targets. *Expert Rev. Anticancer Ther.* **2010**, *10*, 935. [CrossRef]
62. Qian, C.; Lai, C.J.; Bao, R.; Wang, D.G.; Wang, J.; Xu, G.X.; Atoyan, R.; Qu, H.; Yin, L.; Samson, M.; et al. Cancer Network Disruption by a Single Molecule Inhibitor Targeting Both Histone Deacetylase Activity and Phosphatidylinositol 3-Kinase Signaling. *Clin. Cancer Res.* **2012**, *18*, 4104–4113. [CrossRef] [PubMed]
63. Landsburg, D.J.; Barta, S.K.; Ramchandren, R.; Batlevi, C.; Iyer, S.; Kelly, K.; Micallef, I.N.; Smith, S.M.; Stevens, D.A.; Alvarez, M.; et al. Fimepinostat (CUDC-907) in Patients with Relapsed/Refractory Diffuse Large B Cell and High-Grade B-Cell Lymphoma: Report of a Phase 2 Trial and Exploratory Biomarker Analyses. *Br. J. Haematol.* **2021**, *195*, 201–209. [CrossRef]
64. Shulman, D.S.; Vo, K.T.; Balis, F.M.; Lindsay, H.; Bagatell, R.; Place, A.E.; Chi, S.N.; Shusterman, S.; Ezrre, S.; Czaplinski, J.; et al. A Phase 1 Trial of Fimepinostat in Children and Adolescents with Relapsed and Refractory Solid and CNS Tumors. *Cancer Med.* **2025**, *14*, e71417. [CrossRef]
65. Somatilaka, B.N.; Sadek, A.; McKay, R.M.; Le, L.Q. Malignant Peripheral Nerve Sheath Tumor: Models, Biology, and Translation. *Oncogene* **2022**, *41*, 2405. [CrossRef] [PubMed]
66. Shurell, E.; Vergara-Lluri, M.E.; Li, Y.; Tran, L.M.; Nakashima, J.; Barzan, K.; Tam, B.; Bernthal, N.; Tap, W.D.; Eckardt, J.; et al. Correlation of PTEN Loss and PI3K/AKT/MTOR Pathway Upregulation with Malignant Peripheral Nerve Sheath Tumor (MPNST) Development and Outcome. *J. Clin. Oncol.* **2013**, *31*, 10555. [CrossRef]

Disclaimer/Publisher's Note: The statements, opinions and data contained in all publications are solely those of the individual author(s) and contributor(s) and not of MDPI and/or the editor(s). MDPI and/or the editor(s) disclaim responsibility for any injury to people or property resulting from any ideas, methods, instructions or products referred to in the content.